JOC Article
pubs.acs.org/joc

Recognition of Achiral and Chiral Ammonium Salts by Neutral Ditopic Receptors Based on Chiral Salen-UO_2 Macrocycles

Maria E. Amato, Francesco P. Ballistreri, Salvatore Gentile, Andrea Pappalardo, Gaetano A. Tomaselli,* and Rosa M. Toscano

Dipartimento Scienze Chimiche, University of Catania, viale A. Doria 6, 95125 Catania, Italy

gtomaselli@unict.it

Received October 30, 2009

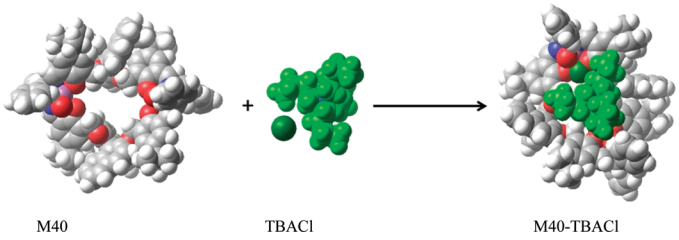

A mononuclear (**M20**) and a dinuclear (**M40**) uranyl chiral macrocyclic complex, incorporating both a salen unit containing two phenyl rings linked to a chiral diimine bridge and the (*R*)-BINOL unit, behaves as an efficient ditopic receptor for achiral and chiral quaternary ammonium salts. Binding affinities in chloroform solution have been measured for 1:1 complexes of many quaternary salts encompassing tetramethylammonium (TMA), tetraethylammonium (TEA), tetrabutylammonium (TBA), and acetylcholine (ACh), as well as trimethylanilinium (TriMAn), benzyltrimethylammonium (BnTriMA), (α-methylbenzyl)trimethylammonium and pyrrolidinium cations. The anion of the salt is bound by the hard Lewis acidic uranyl site, with an increasing binding efficiency on increasing the anion hardness ($I^- < Br^- < Cl^-$), whereas CH−π or π−π attractions by binapthyl moiety, or the salicylaldehyde unit, or the phenyl rings of diimine bridge ensure the recognition of the cation partner. Optimized structures of receptor−anion−cation ternary complexes obtained by MM calculations are supported by 2D-ROESY NMR measurements.

Introduction

The design and synthesis of chiral macrocyclic cavities acting as enantioselective receptors is a topic of great interest in the field of enzyme mimicking enantioselective catalysis as well as of chiral resolution and chiral sensing.[1] Recently particular attention has been devoted to heteroditopic receptor systems able to coordinate simultaneously both anionic and cationic guest species.[2] Different strategies are followed to bind the anion and the corresponding cation separately within the receptor. Thus, the anion is bound by Lewis acidic coordination sites or by electrostatic ion−dipole or hydrogen bonding interactions, whereas the cation may be bound by some common systems such as crown ethers or, if it is an organic cation, π-electron rich molecules developing cation−π interactions.[2b,3] In organic solvents of low polarity a contact ion pair binding process would be the

(1) (a) Beer, P. D.; Gale, P. A. *Angew. Chem., Int. Ed.* **2001**, *40*, 486. (b) Thomas, C. M.; Ward, T. R. *Chem. Soc. Rev.* **2005**, *34*, 337. (c) Ballester, P.; Vidal-Ferran, A. in *Supramolecular Catalysis*; Van Leeuwen, P. W. N. M, Ed.; Wiley-VCH Verlag: Weinheim, Germany, 2008; p 1.

(2) (a) Pelizzi, N.; Casnati, A.; Friggeri, A.; Ungaro, R. *J. Chem. Soc., Perkin Trans. 2* **1988**, 1307. (b) Antonisse, M. M.; Reinhoudt, D. N. *Chem. Commun.* **1998**, 443. (c) White, D.; Laing, N.; Miller, H.; Parsons, S.; Coles, S.; Tasker, P. A. *Chem.Commun.* **1999**, 2077. (d) Evans, A. J.; Beer, P. D. *Dalton Trans.* **2003**, 4451. (e) Cametti, M.; Nissinen, M.; Dalla Cort, A.; Mandolini, L.; Rissanen, K. *Chem. Commun.* **2003**, 2420. (f) Mahoney, J. M.; Nawaratna, G. U.; Beatty, A. M.; Duggan, P. J.; Smith, B. D. *Inorg. Chem.* **2004**, *43*, 5902 and references cited therein. (g) Cametti, M.; Nissinen, M.; Dalla Cort, A.; Mandolini, L.; Rissanen, K. *J. Am. Chem. Soc.* **2007**, *129*, 3641. (h) Smith, B. D. In *Ion Pair Recognition by Ditopic Receptors, Macrocyclic Chemistry: Current Trends and Future*; Gloe, K., Antonioli, B., Eds.; Kluwer: London, UK, 2005; p 137. (i) Steed, J. W.; Atwood, J. L. *Supramolecular Chemistry*; Wiley: London, UK, 2000.

(3) (a) Kubik, S. *J. Am. Chem. Soc.* **1999**, *121*, 5846. (b) Kubik, S.; Goddard, R. *Chem. Commun.* **2001**, 633. (c) Masci, B.; Persiani, D.; Thuéry, P. *J. Org. Chem.* **2006**, *71*, 9784. (d) Masci, B.; Levi Mortera, S.; Persiani, D.; Thuéry, P. *J. Org. Chem.* **2006**, *71*, 504. (e) De Iasi, G.; Masci, B. *Tetrahedron Lett.* **1993**, *34*, 6635. (f) Masci, B. *Tetrahedron* **1995**, *51*, 5459. (g) Masci, B.; Finelli, M.; Varrone, M. *Chem.—Eur. J* **1998**, *4*, 2018. (h) Dalla Cort, A.; Mandolini, L.; Pasquini, C.; Schiaffini, L. *Org. Lett.* **2004**, *6*, 1697.

DOI: 10.1021/jo902328y Published on Web 02/09/2010
© 2010 American Chemical Society

CHART 1. Chemical Formulas of Receptors M20 and M40

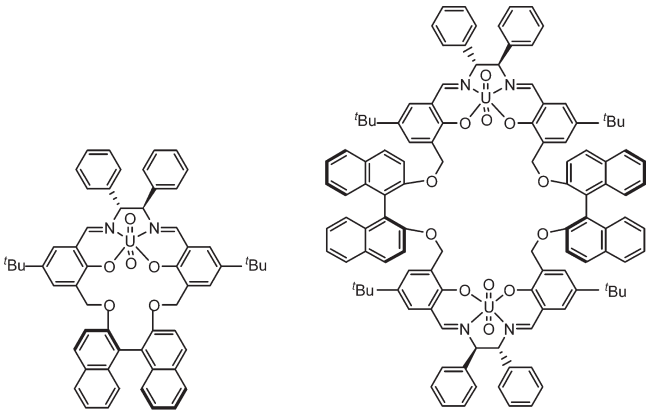

preferred recognition pathway because this avoids the energetically unfavorable separation of the two ions. A further important feature is the geometry of the ditopic receptor that must ensure the optimum distance between cation and anion sites in order to maintain a strong cation−anion interaction. In a previous paper we have reported the synthesis and the conformational aspects of mononuclear (**M20**) and dinuclear (**M40**) uranyl chiral macrocyclic complexes (Chart 1) incorporating both a salen unit containing a chiral diimine bridge and the (*R*)-BINOL unit.[4]

The salen framework, because of the presence of two stereogenic carbon atoms in the diimine bridge, generates a chiral pocket that, via imine nitrogen and phenolic oxygen atoms, can coordinate the uranyl dication, creating therefore a Lewis acidic site that can bind the counteranion of an ion pair. A pentagonal bipyramidal coordination geometry for uranyl(VI) ion with two axial oxo groups and with the fifth equatorial site available for complexation with anionic monodentate ligands X^- has been previously indicated in these uranyl chiral macrocyclic complexes.[4,5] On the other hand, the (*R*)-BINOL unit can provide π electron-rich regions able to develop CH$-\pi$ interactions, thus facilitating the recognition of the countercation of the ion pair. Also the geometrical requisites can be satisfied by the adopted **M20** and **M40** conformations. Therefore we tested the ability of these two uranyl complexes to work as neutral ditopic receptors toward both achiral and chiral ammonium salts.

Results and Discussion

Achiral Ammonium Salts. Binding constants for 1:1 complexes of achiral quaternary ammonium salts Q^+X^- listed in Chart 2 with **M20** and **M40** receptors (Chart 1) respectively were obtained in $CDCl_3$ at 27 °C from ^{1}H NMR titrations, monitoring the time averaged proton signals of the onium Q^+ cations as a function of increasing receptor concentration. Both receptor and onium salt chemical shifts were independent of concentration (0.1−5 mM) thereby excluding possible aggregation effects. Generally, the addition of increasing amounts of ammonium salt to the uranyl receptor

CHART 2. Chemical Formulas of Achiral Ammonium Salt Guests

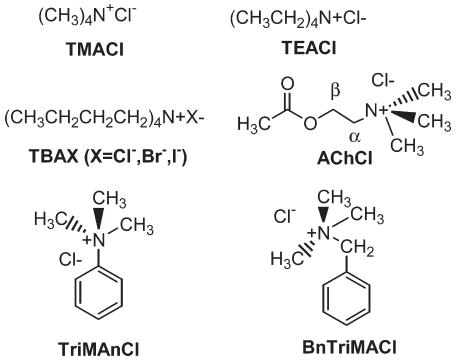

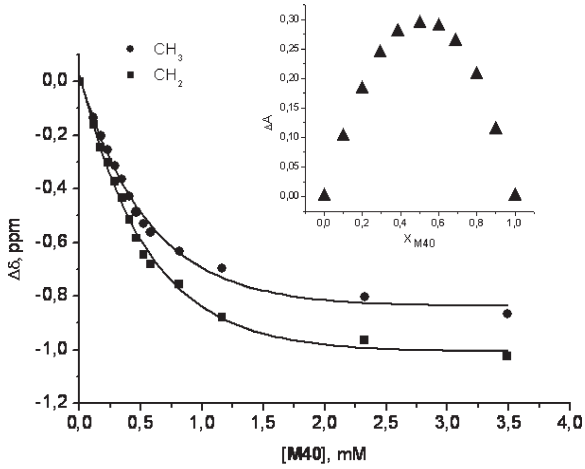

FIGURE 1. ^{1}H NMR of 1 mM TEACl with receptor **M40** in $CDCl_3$ at 27 °C. The inset displays the corresponding Job plot.

caused considerable and reproducible upfield shifts ($\Delta\delta$) of the protons of NCH_3, NCH_2-, and NCH_2Ar groups of the Q^+ cations. Likewise, also the signals of the host underwent significant shifts. In particular, the OCH_2 methylene protons of both **M20** and **M40** receptors were the most affected and displayed appreciable downfield shifts. A representative example of a titration curve is shown in Figure 1, together with the corresponding Job plot.[6]

Titration data were fitted to a 1:1 binding isotherm even in the case of **M40** receptor (which has two potential binding sites) by using an iterative procedure, from which the binding constants (K, M^{-1}) and limiting upfield shifts ($-\Delta\delta_\infty$, ppm) as best fit parameters were obtained.[7] Multiple titration plots were in all cases internally consistent (see the Supporting Information).

Table 1 displays the binding constant K values and limiting upfield shifts $-\Delta\delta_\infty$ relative to the formation of complexes between **M20** and **M40** uranyl-salen receptors and some achiral tetraalkylammonium salts. The data obtained indicate that in all cases **M40** is a better receptor than **M20**, which generally is not able to form very strong complexes. The best guest for **M20** is tetramethylammonium chloride (TMACl)

(4) Amato, M. E.; Ballistreri, F. P.; Pappalardo, A.; Sciotto, D.; Tomaselli, G. A.; Toscano, R. M. *Tetrahedron* **2007**, *63* (39), 9751.
(5) Amato, M. E.; Ballistreri, F. P.; Pappalardo, A.; Tomaselli, G. A.; Toscano, R. M.; Williams, J. D. *Eur. J. Org. Chem.* **2005**, 3562.
(6) Georghiou, P. E.; Tran, A. H.; Mizyed, S.; Bancu, M.; Scott, L. T. *J. Org. Chem.* **2005**, *70*, 6158.
(7) Cattani, A.; Dalla Cort, A.; Mandolini, L. *J. Org. Chem.* **1995**, *60*, 8313.

TABLE 1. Binding Constants (K, M^{-1}) and Limiting Upfield Shifts ($-\Delta\delta_\infty$, ppm) for Complexes of Achiral Quaternary Ammonium Salts with Receptors M20 and M40

		M20		M40	
entry	Q^+X^- [a]	K	$-\Delta\delta_\infty$	K	$-\Delta\delta_\infty$
1	TMACl	1512 ± 351	0.39 (NCH_3)	3354 ± 465	1.44 (NCH_3)
2	TriMAnCl	476 ± 42	1.93 (NCH_3)	707 ± 83	1.71 (NCH_3)
3	BnTriMACl			621 ± 81	1.32 (NCH_3)
4	TBACl	169 ± 15	1.5 (CH_3)	20826 ± 1011	0.51 (CH_3)
5	TBABr			1574 ± 130	0.29 (CH_3)
6	TBAI			808 ± 126	0.038 (CH_3)
7	TEACl	175 ± 68	2.2 (NCH_2)	1731 ± 150	1.03 (CH_3);1.23(NCH_2)
8	AChCl	112 ± 3	1.39 (NCH_3)	2568 ± 534	1.08 (NCH_3)

[a] Q^+X^- concentrations in the titration experiments were in the range 0.1−5 mM.

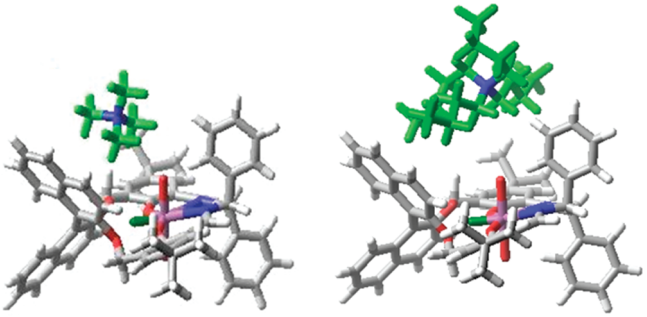

FIGURE 2. Optimized structures of **M20**−TMACl and **M20**−TBACl complexes.

(entry 1) followed by trimethylanilinium chloride (TriMAnCl) (entry 2) with a K value that is nearly one-third that of TMACl ($K_{TMACl}/K_{TriMAnCl}$ = 3.2). Increasing the alkyl group size as in the case of tetrabutylammonium chloride (TBACl) (entry 4) and tetraethylammonium chloride (TEACl) (entry 7) lowers the pertinent K constants dramatically to values about ten times smaller than the TMACl K value (K_{TMACl}/K_{TBACl} = 8.9). Similar behavior is observed also for acetylcholine chloride (AChCl; entry 8; K_{TMACl}/K_{AChCl} = 13). The observed predilection of **M20** receptor for the TMACl guest might be explained on the basis of its cavity size and on the bulkiness of the different guests.

MacroModel MM Optimized Structures. To verify this hypothesis molecular mechanics calculations were carried out, using the MM2* force field of MacroModel 8.6,[8] to obtain optimized structures of the receptor−anion−cation ternary complexes formed (Figure 2). The cavity size estimated for the **M20** receptor by molecular mechanics optimized structure is nearly 5 Å and therefore it is not suitable to accommodate larger guests such as TBACl but rather it matches well with the shape and the size of TMACl (4.5 Å).

The shorter calculated host−guest equilibrium distance for the **M20**−TMACl complex implies stronger interactions than for the **M20**−TBACl complex and therefore higher affinity. It is worth noting in the case of TMACl the significant role played by the binaphtyl moiety as well as by that of the salicylaldehyde unit and of a phenyl ring of the diimine bridge in building up a π-rich cavity that is involved in stabilizing CH−π interactions. On the contrary TBACl,

(8) Mohamadi, F.; Richards, N. G. J.; Guida, W. C.; Liskamp, R.; Lipton, M.; Caufield, C.; Chang, G.; Hendrickson, T.; Still, W. C. *J. Comput. Chem.* **1990**, *11*, 440.

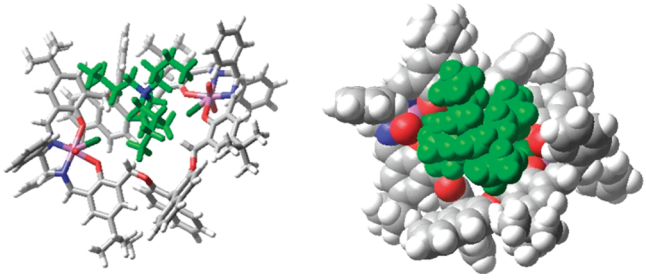

FIGURE 3. Optimized structure of 1:1 **M40**−TBACl complex.

which is the worst guest with **M20**, appears the best guest with **M40**, having a K value that is nearly 2 orders of magnitude higher than the corresponding K value observed with **M20** (entry 4). For TBACl a size of 9 Å can be estimated. On the other hand the cavity of M40 has a size close to 10 Å, which is larger than that of **M20** (∼5 Å). Therefore TBACl is able to fit well the **M40** cavity (Figure 3); hence various and stronger CH−π interactions arise among the π rich regions of **M40** and the CH groups of the guest, CH−π interactions which, on the contrary, do not occur or are less significant in the case of **M20**. As the optimized structure shows also in this case, an important role in establishing cation/π interactions is played by the salicylaldehyde and binaphthyl moieties of the **M40** receptor. The three guests TBACl, TEACl, and AChCl which display similar and lower affinity toward the smaller **M20** receptor, in contrast with the larger **M40** receptor, yield complexes of different and higher stability. The observed selectivity (K_{TBACl}/K_{TEACl} = 12, K_{TBACl}/K_{AChCl} = 8) is presumably due to a larger number of and more efficient CH−π interactions involved in the recognition process of TBACl than TEACl and AChCl (Figure 4). Salts bearing an aromatic ring, such as TriMAnCl and BnTriMACl (entries 2 and 3), were also employed as guests in order to evaluate the contribution of π−π interactions on the binding affinities. The similar K values observed for these two guests with the receptor **M40**, which are lower than the K value observed for TMACl with **M40** itself (entry 1), seem to indicate that replacing a methyl group of the cation (TMACl) with a phenyl (TriMAnCl) or a benzyl group (BnTriMACl) respectively leads to a lower binding constant and affinity and indicates a minimal role played with these guests by the π−π stacking interactions compared to that of CH−π interactions.

The binding efficiency of TBA salts increases on increasing the counteranion hardness passing from iodide to bromide and to chloride (entries 4−6) ($I^- < Br^- < Cl^-$, K_{TBACl}/K_{TBABr} = 13, K_{TBABr}/K_{TBAI} = 1.9) according to the hard Lewis acidic

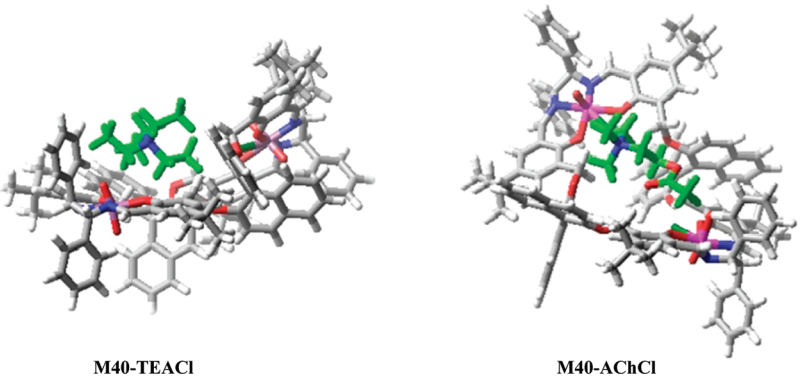

FIGURE 4. Optimized structures of 1:1 **M40**−TEACl and 1:1 **M40**−AChCl complexes.

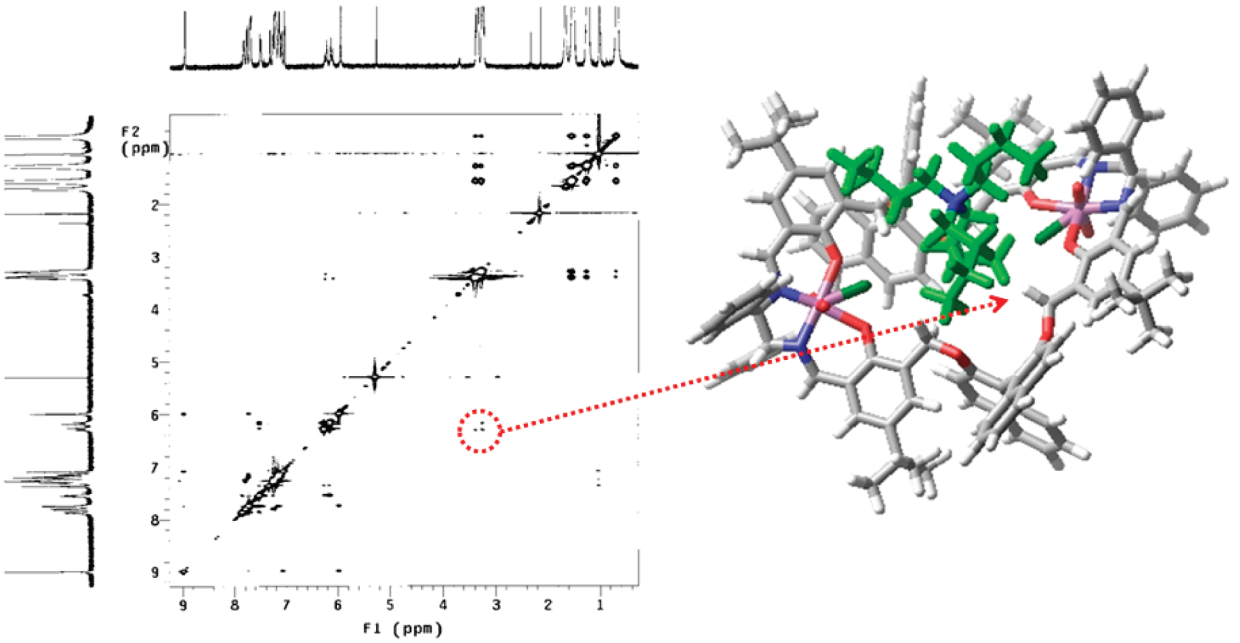

FIGURE 5. T-ROESY map of **M40**−TBACl complex in $CDCl_3$ solution.

character of the uranyl center and supporting the idea that the driving force of the binding event is based on the initial strong interaction of the hard chloride ion with the hard Lewis acidic nature of the uranyl center.

2D T-ROESY Experiments. To have solid state structures, efforts were made to obtain suitable crystals of **M40**−TBACl and **M40**−AChCl host−guest complexes by adopting the slow evaporation technique of solutions.[2g] Unfortunately attempts failed in all cases. Therefore, in order to obtain some structural information for these two complexes 2D T-ROESY experiments were performed. The spectra obtained in $CDCl_3$ solution for both **M40**−TBACl and **M40**−AChCl complexes showed dipolar correlation cross peaks between the OCH_2 protons of the receptor and the *N*-methylene and *N*-methyl hydrogens of the salt. The presence of these ROE contacts implies a close proximity between the receptor and the ammonium group and, basically, seems good evidence for the formation of complexes with the ammonium cation located inside the receptor nearby the uranyl site (Figures 5 and 6). As further support for this conclusion, upon complexation we observed splitting of the N-bonded methylene protons of TBACl, which resonate as a well-resolved AB system ($\Delta\delta$ = 0.1 ppm), indicating that binding causes the loss of conformational freedom of the butyl chains. Therefore the optimized structures, which seem consistent with the NMR measurements, make clear the important role played by the (*R*)-BINOL unit in allowing CH−π interactions which give a large contribution in determining the affinity of the quaternary salt for the receptor. Furthermore, these calculated structures support the observed downfield chemical shift of OCH_2 methylene protons of receptor as a probe of the location of cation guest in the complex, and emphasize the selection operated by cavity size toward guests of different bulkiness.

Chiral Ammonium Salts. Binding affinities of some chiral ammonium iodides (Chart 3) for the **M40** receptor have been determined in chloroform solution. Also in this case 1:1 complexes were obtained as shown by the pertinent Job plots (see the Supporting Information). We have chosen two parent ammonium salts, i.e., (α-methylbenzyl)trimethylammonium iodide and 2-anilinomethyl-1-ethylmethylpyrrolidinium iodide. In the first compound only the benzylic carbon atom is a stereocenter and therefore we have studied the affinities of the two enantiomeric ammonium salts (***R*-1** and ***S*-1**) for

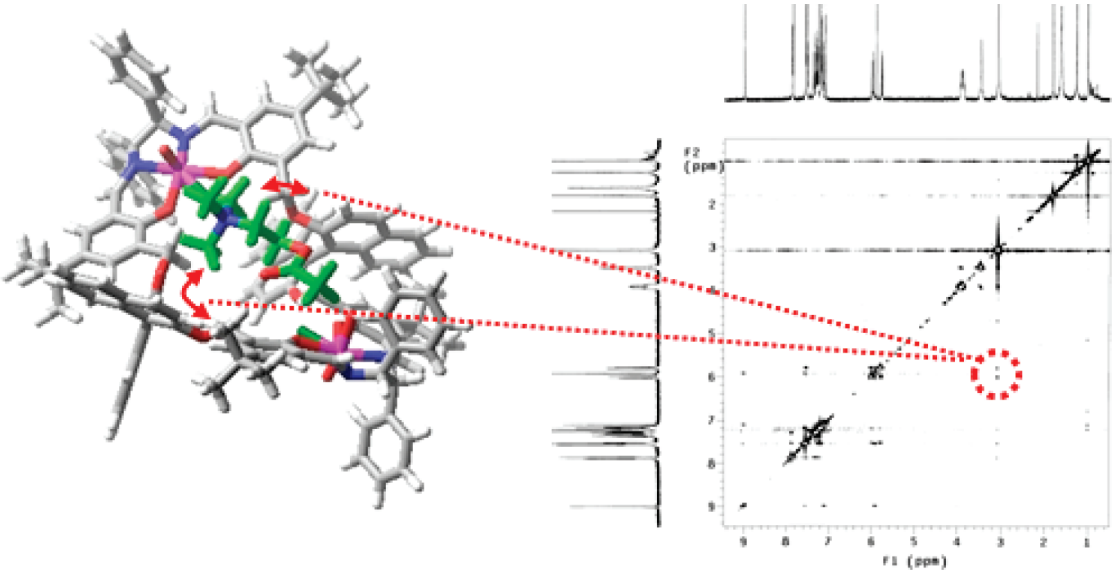

FIGURE 6. T-ROESY map of **M40**−AChCl complex in $CDCl_3$ solution.

CHART 3. Chemical Formulas of Chiral Ammonium Salt Guests

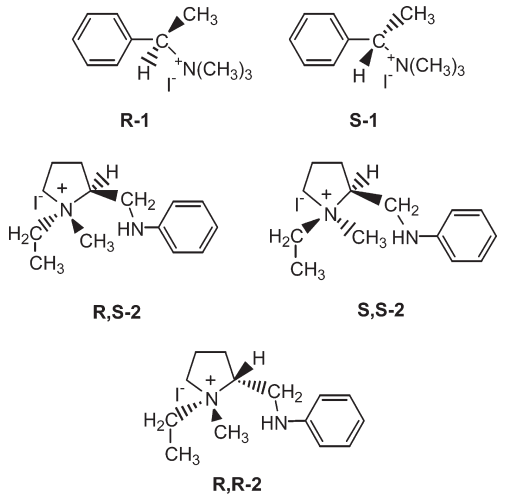

M40. In the other substrate both the ring-nitrogen and the carbon atom in position 2 of the proline ring are stereocenters and thus four isomers, two pairs of enantiomers and two pairs of diastereomers, are possible. We have determined the affinities for three of the four possible isomers, i.e., two pairs of diastereomers (***R*,*S*-2**)/(***S*,*S*-2**) and (***R*,*S*-2**)/(***R*,*R*-2**) and a pair of enantiomers (***S*,*S*-2**)/(***R*,*R*-2**); we were not able to isolate the fourth isomer (*R*-2-anilinomethyl-*S*-1-ethylmethylpyrrolidinium iodide) with high purity (see the Supporting Information). The relative binding constants are reported in Table 2.

For both the enantiomers of (α-methylbenzyl)trimethylammonium iodide, different chemical shift changes were observed upon addition of **M40** receptor to each enantiomer as a result of the formation of diastereomeric molecular complexes. A comparison between the observed binding constants of BnTriMACl (entry 3, Table 1) and those of *R*- and *S*-(α-methylbenzyl)trimethylammonium iodides (entries 1 and 2, Table 2) respectively indicates that the replacement

TABLE 2. Binding Constants (K, M^{-1}) and Limiting Upfield Shifts ($-\Delta\delta_\infty$, ppm) for Complexes of Chiral Quaternary Ammonium Salts with Receptors M40

		M40		
entry	Q^+I^-	K	$-\Delta\delta_\infty$	enantioselectivity
1	***R*-1**	968 ± 115	1.45 (NCH_3)	$K_{S\text{-}1}/K_{R\text{-}1}$ = 1.7
2	***S*-1**	1668 ± 135	1.25 (NCH_3)	
3	***R*,*S*-2**	3323 ± 338	0.31 (NCH_3)	
4	***S*,*S*-2**	3092 ± 462	0.92 (NCH_3)	$K_{R,R\text{-}2}/K_{S,S\text{-}2}$ = 2.5
5	***R*,*R*-2**	7847 ± 687	0.85 (NCH_3)	

of a benzylic hydrogen atom of BnTriMACl with a methyl group and the subsequent generation of a stereocenter makes the affinity of the iodide for **M40** slightly higher than that of BnTriMACl itself ($K_{R\text{-}1}/K_{\mathrm{BnTriMACl}}$=1.5), if the carbon atom stereocenter has the (*R*)-configuration (entry 1, Table 2). The iodide affinity results are 3-fold higher ($K_{S\text{-}1}/K_{\mathrm{BnTriMACl}}$ = 2.7) if the carbon atom stereocenter has the (*S*)-configuration (entry 2, Table 2), even if chlorides usually form much more stable complexes than iodides. In other words the expected lowering in affinity for receptor **M40** by replacing the counteranion chloride with iodide is largely counterbalanced by the introduction of a stereocenter in the guest framework, which is responsible for the generation of new host−guest interactions (CH−π or π−π interactions). The ratio $K_{S\text{-}1}/K_{R\text{-}1}$ = 1.7 indicates that **M40** is able to discriminate the two enantiomers. The lower affinity of compound ***R*-1** is due to the configuration of the stereocenter, which does not let the phenyl ring have the optimal orientation to establish π−π interactions with the aromatic binaphthyl moiety of the host. Therefore only less important but still significant CH−π interactions occur. On the other hand, as the optimized structures of these complexes show (Figure 7), the phenyl ring of ***S*-1** can be located in a favorable spatial disposition to establish π−π interactions with the binaphthyl unit of the host and then a higher affinity for **M40** receptor is observed.

In the case of proline derivatives the affinity values observed for the two diastereomers ***R*,*S*-2** and ***S*,*S*-2** are nearly

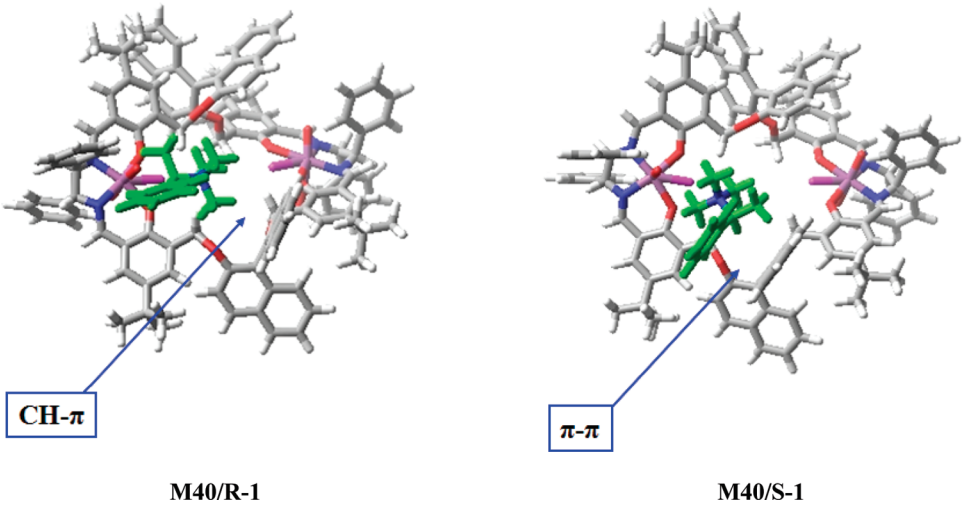

FIGURE 7. Optimized structures of 1:1 **M40**/***R*-1** and 1:1 **M40**/***S*-1** complexes.

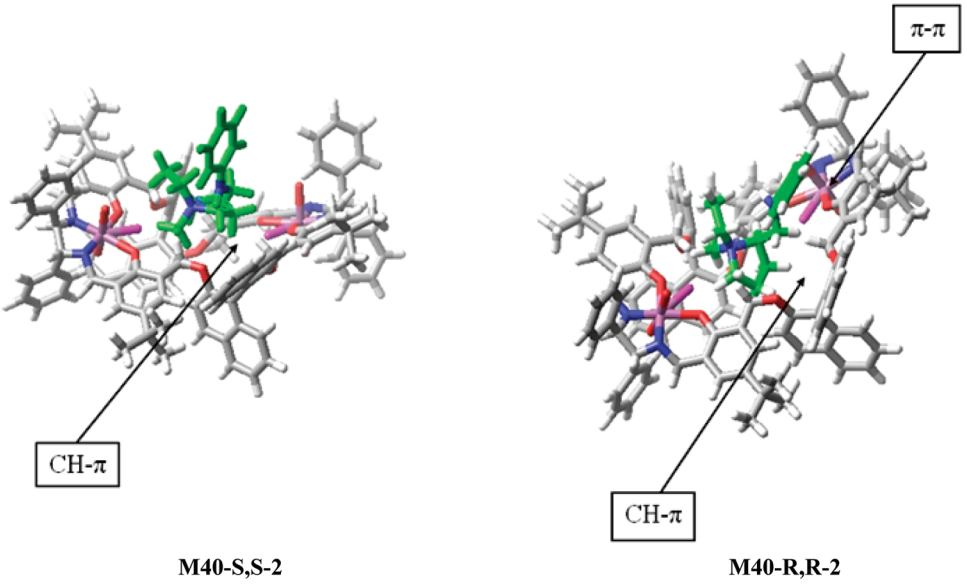

FIGURE 8. Optimized structures of 1:1 **M40**−***S*,*S*-2** and 1:1 **M40**−***R*,*R*-2** complexes.

equal and within the experimental errors ($K_{R,S\text{-}2}/K_{S,S\text{-}2}$ = 1.1). This observation can be considered as evidence that the change of configuration of the nitrogen atom stereocenter does not play a relevant role in the molecular recognition mechanism. Additional support for this conclusion comes from the observation that a selective process is occurring with diastereomers ***R*,*R*-2**/***R*,*S*-2** ($K_{R,R\text{-}2}/K_{R,S\text{-}2}$ = 2.4), which differ only for the configuration at the carbon atom. Likewise, chiral selection is now observed for the two enantiomers ***R*,*R*-2**/***S*,*S*-2** ($K_{R,R\text{-}2}/K_{S,S\text{-}2}$ = 2.5), where the larger contribution to the selection is due to the presence of the carbon atom stereocenter. Optimized structures of these complexes (Figure 8) are useful in understanding such a behavior. In fact, the change of configuration of the nitrogen atom of the proline ring (obtained by exchanging the position of the methyl group with that of the ethyl group) does not imply substantial modifications of host−guest interactions. On the other hand, the change of configuration of the carbon atom in the case of the ***R*,*R*-2** enantiomer leads to $\pi-\pi$ interactions (between the phenyl ring of the aniline framework and that of the binaphthyl unit), interactions which are presumably less important for the ***S*,*S*-2** enantiomer.

Conclusion

In summary, the two uranyl chiral macrocyclic complexes **M20** and **M40** are able to work as selective neutral ditopic receptors toward both achiral and chiral ammonium salts. **M20** and **M40** are able to discriminate achiral ammonium salts on the basis of different CH$-\pi$ interactions between the cation and the binaphthyl moiety, the salicylaldehyde unit, and the phenyl rings of the diimine bridge present in the receptor. The selective recognition is controlled by receptor cavity sizes: guests with less than 5 Å bulkiness are recognized by **M20**, whereas guests larger than 5 Å are better recognized by **M40**. On the other hand, the **M40** chiral receptor is able to perform chiral recognition toward chiral ammonium iodide salts on the basis of different host−guest interactions, due to matching or mismatching of host−guest chirality.

Experimental Section

Materials. Trimethylphenylammonium chloride, benzyltrimethylammonium chloride, tetrabutylammonium chloride, tetrabutylammonium bromide, tetrabutylammonium iodide, acetylcholine chloride, tetraethylammonium chloride, tetramethylammonium chloride, (*R*)-(+)-1-phenylethylamine, (*S*)-(−)-1-phenylethylamine, (*R*)-proline, and (*S*)-proline were commercially available reagent-grade materials and were used without further purification. NMR experiments were carried out at 27 °C on a 500 MHz spectrometer (^{1}H at 499.88 MHz, ^{13}C NMR at 125.7 MHz) equipped with a pulse field gradient module (Z axis) and a tunable 5 mm Varian inverse detection probe (ID-PFG). Unless otherwise stated, NMR spectra were obtained in $CDCl_3$ solutions. The chemical shifts (ppm) were referenced to TMS. A UV/vis spectrophotometer equipped with a 1 cm path-length cell was used for the determination of Job plots. ESI-MS spectra were obtained by employing an ES-MS spectrometer equipped with an ion trap analyzer. The (*R*)-(+)- and (*S*)-(−)-trimethyl-1-phenylethylammonium iodides were prepared according to a literature procedure.[9]

The syntheses of the macrocycles and their uranyl complexes are reported elsewhere.[4]

(*R*)- or (*S*)-Acetylproline. (*R*)- or (*S*)- acetylproline was prepared by a slight modification of a literature procedure.[10] A mixture of (*R*)- or (*S*)-proline (2.53 g, 22 mmol) and acetic anhydride (4.2 mL, 44 mmol) in ethyl acetate (44 mL) was sonicated for 10 min at room temperature. At the end of the reaction, the solvent was evaporated and the residue dried under vacuum (3.34 g, 21.2 mmol, 96% yield, mp 111−113 °C). ^{1}H NMR (500 MHz, $CDCl_3$) δ 1.95 (m, 1H), 2.04 (m, 2H), 2.18 (s, 3H), 2.56 (m, 1H), 3.47(m, ^{1}H), 3.58 (m, 1H), 4.61−4.63 (dd, J= 8.0, 1.7 Hz, 1H); ^{13}C NMR (125 MHz, $CDCl_3$) δ 22.1, 24.7, 27.9, 48.4, 59.6, 172.3, 172.8.

(*R*)- and (*S*)-Acetylprolinanilide. (*R*)- and (*S*)-acetylprolinanilide were prepared as reported in the literature.[11] ^{1}H NMR (500 MHz, $CDCl_3$) δ 1.82 (m, 1H), 2.05 (m, 1H), 2.15 (s, 3H), 2.19 (m, 1H), 2.62 (m, 1H), 3.46 (m, 1H), 3.56 (m, 1H), 4.78 (d, J = 7.6 Hz, 1H), 7.06 (t, J = 7.6 Hz, 1H), 7.29 (t, J = 8.05 Hz, 2H), 7.53 (d, J = 8.05 Hz, 1H), 9.66 (br s, 1H).

(*R*)- and (*S*)-Anilinomethyl-1-ethylpyrrolidine. (*R*)- and (*S*)-anilinomethyl-1-ethylpyrrolidine were prepared as reported in the literature.[11] ^{1}H NMR (500 MHz, $CDCl_3$) δ 1.11 (t, J=7.3 Hz, 3H), 1.77 (m, 3H), 1.91 (m, 1H), 2.22 (m, 2H), 2.68 (m, 1H), 2.85 (m, 1H), 3.10 (m, 1H), 3.23 (m, 2H), 4.26 (br s, 1H), 6.62 (d, J = 7.6 Hz, 1H), 6.67 (t, J = 7.32 Hz, 2H), 7.17 (t, J = 7.32 Hz, 2H).

(*S*)-2-Anilinomethyl-(*S*)-1-ethylmethylpyrrolidinium Iodide (*S*,*S*-2) and (*S*)-2-Anilinomethyl-(*R*)-1-ethylmethylpyrrolidinium Iodide (*R*,*S*-2). CH_3I (1.25 mL, 20 mmol) was added under N_2 to a stirred solution of (*S*)-2-anilinomethyl-1-ethylpyrrolidine (600 mg, 3 mmol) in CH_2Cl_2. The reaction was monitored by TLC ($CH_3OH/CHCl_3$, 9:1). During the reaction a white precipitated formed. After the disappearance of the substrate (48 h) the precipitate was filtered and washed with CH_2Cl_2 (420 mg, 1.21 mmol, 40% yield). ^{1}H NMR and ESI-MS measurements indicated that the precipitate was the (*S*)-2-anilinomethyl-(*S*)-1-ethylmethylpyrrolidinium iodide (***S*,*S*-2**) (see the Supporting Information). ^{1}H NMR (500 MHz, $CDCl_3$) δ 1.40 (t, J = 7.3 Hz, 3H), 2.01 (m, 1H), 2.18 (m, 1H), 2.29 (m, 1H), 2.57 (m, 1H), 3.20 (s, 3H), 3.59 (m, 3H), 3.75 (m, 1H), 3.84 (m, 1H), 4.23 (m, 1H), 4.48 (m, 1H), 5.38 (br s, 1H), 6.74 (d, J = 7.5 Hz, 2H), 6.77 (dd, J = 7.5 Hz, 1H), 7.20 (dd, J = 7.5 Hz, 2H). Anal. Calcd for $C_{14}H_{23}IN_2$: C, 48.54; H, 6.70; N, 8.09. Found: C, 48.43; H, 6.64; N, 8.01.

The solution obtained after filtration was dried ($MgSO_4$) and evaporated under vacuum to give a white solid (400 mg, 1.16 mmol, 39% yield). The solid obtained is a mixture of the two diastereomers ***S*,*S*-2** and ***R*,*S*-2**. The separation of the two diastereomers was based on their different solubilities in water and in CH_2Cl_2. Therefore the solid was washed several times with water until NMR measurements indicated that it was a pure sample of (*S*)-2-anilinomethyl-(*R*)-1-ethylmethylpyrrolidinium iodide (***R*,*S*-2**). ^{1}H NMR (500 MHz, $CDCl_3$) δ 1.37 (t, J = 7.3 Hz, 3H), 2.03 (m, 1H), 2.24 (m, 2H), 2.53 (m, 1H), 3.19 (s, 3H), 3.60 (m, 3H), 3.67 (m, 1H), 3.81 (m, 1H), 4.16 (m, 1H), 4.34 (m, 1H), 5.37 (br s, 1H), 6.75 (d, J = 7.5 Hz, 2H), 6.77 (dd, J = 7.5 Hz, 1H), 7.18 (dd, J = 7.5 Hz, 2H). Anal. Calcd for $C_{14}H_{23}IN_2$: C, 48.54; H, 6.70; N, 8.09. Found: C, 48.75;, H, 6.67; N, 8.08. ESI-MS shows the molecular ion peak of the expected compound.

(*R*)-2-Anilinomethyl-(*R*)-1-ethylmethylpyrrolidinium Iodide (*R*,*R*-2). The previous experimental procedure was followed for the reaction of (*R*)-2-anilinomethyl-1-ethylpyrrolidine with CH_3I. Unfortunately in this case only the isomer (*R*)-2-anilinomethyl-(*R*)-1-ethylmethylpyrrolidinium iodide was obtained as a pure compound. The product was characterized by NMR, ESI-MS, and 2-D NMR NOESY measurements (see the Supporting Information). ^{1}H NMR (500 MHz, $CDCl_3$) δ 1.40 (t, J = 7.3 Hz, 3H), 2.01 (m, 1H), 2.18 (m, 1H), 2.29 (m, 1H), 2.57 (m, 1H), 3.20 (s, 3H), 3.59 (m, 3H), 3.75 (m, 1H), 3.84 (m, 1H), 4.23 (m, 1H), 4.48 (m, 1H), 5.38 (br s, 1H), 6.74 (d, J = 7.5 Hz, 2H), 6.77 (dd, J = 7.5 Hz, 1H), 7.20 (dd, J = 7.5 Hz, 2H). Anal. Calcd for $C_{14}H_{23}IN_2$: C, 48.54; H, 6.70; N, 8.09. Found: C, 48.80; H, 6.63; N, 8.06.

Acknowledgment. We thank the University of Catania for financial support.

Supporting Information Available: ^{1}H NMR titrations and Job plots, 1D and 2D-NMR spectra, 2D-NMR NOESY, and synthesis of proline isomers. This material is available free of charge via the Internet at http://pubs.acs.org.

(9) Guijarro, D.; Martinez, P. J.; Najera, C.; Yus, M. *Arkivoc* **2004**, *iv*, 5.
(10) Anuradha, M. V.; Ravindranath, B. *Tetrahedron* **1997**, *53*, 1123.
(11) Suzuki, K.; Igekawa, A.; Mukajyama, T. *Bull. Chem. Soc. Jpn.* **1982**, *55*, 3277.